ルまたは中心静脈ポートを留置し，5-FUを持続静注するほうが望ましい．

IV．有害事象および副作用

FOLFOX 4レジメンのおもな有害事象および副作用は，①末梢神経障害，②消化器症状(悪心，嘔吐，下痢，口内炎，食欲不振，腹痛，便秘など)，③疲労，④脱毛，⑤咳嗽，⑥骨髄抑制(白血球減少，好中球減少，貧血，血小板減少)，⑦GOT/GPT上昇などである．末梢神経障害は80～90%に認められ，冷たいものに接触することで誘発あるいは悪化する四肢末端や口唇周囲の知覚不全，感覚異常(しびれなど)である．

感覚異常による機能障害(立つ，歩く，物を持つ，ボタンをかけるなどの動作において困難を伴う)を認めることがあり，この症状はL-OHPの累積投与量に依存して発現する．累積投与量540 mg/m^{2}で約1%，780 mg/m^{2}で約20%，1,170 mg/m^{2}で約40%にみられる．ほとんどの有害事象や副作用は休薬期間に回復，軽快する．しかし，重篤な下痢や好中球減少の出現時には止痢剤，補液，顆粒球コロニー刺激因子(G-CSF)製剤などを適切に使用する．

おわりに

欧米における切除不能進行・再発結腸・直腸癌に対する治療成績は，CPT-11とL-OHPの有効な使用により初回治療の奏効率で40%以上，生存期間中央値で20カ月以上と格段の進歩を遂げた．わが国でもL-OHPが承認された今日，日本人におけるFOLFOXレジメンの有効性と安全性を確認し，さらに経口フッ化ピリミジン系薬剤や分子標的薬剤(bevacizumab，cetuximabなど)との併用療法を早急に検討する必要がある．

参考URL

1) NCI homepage：
http://www.nci.nih.gov/cancerinfo/pdq/treatment/colon/healthprofessional/

文　献

1) Tournigand, C., André, T., Achille, E., et al.：FOLFIRI followed by FOLFOX 6 or the reverse sequence in advanced colorectal cancer：a randomized GERCOR study. J. Clin. Oncol. 22；229-237, 2004
2) de Gramont, A., Figer, A., Seymour, M., et al.：Leucovorin and fluorouracil with or without oxaliplatin as first-line treatment in advanced colorectal cancer. J. Clin. Oncol. 18；2938-2947, 2000
3) Goldberg, R. M., Sargent, D. J., Morton, R. F., et al.：A randomized controlled trial of fluorouracil plus leucovorin, irinotecan, and oxaliplatin combinations in patients with previously untreated metastatic colorectal cancer. J. Clin. Oncol. 22；23-30, 2004
4) Rothenberg, M. L., Oza, A. M., Bigelow, R. H., et al.：Superiority of oxaliplatin and fluorouracil-leucovorin compared with either therapy alone in patients with progressive colorectal cancer after irinotecan and fluorouracil-leucovorin：interim results of a phase III trial. J. Clin. Oncol. 21；2059-2069, 2003
5) Hyodo, I., Shirao, K., Boku, N., et al.：Phase II trial and pharmacokinetic analysis of oxaliplatin(L-OHP) as second-line treatment in patients(pts) with metastatic colorectal cancer(MCRC). Proc. Am. Soc. Clin. Oncol. 21；1383(abst.), 2003
6) Miyata, Y., Shirao, K., Ohtsu, A., et al.：Oxaliplatin(L-OHP) in combination with 5-fluorouracil(5-FU)/*l*-leucovorin(*l*-LV) on modified Roswell Park regimen as first-line treatment of advanced colorectal cancer (ACRC)：A phase I/II study. Proc. Am. Soc. Clin. Oncol. 22；3705(abst.), 2004

Clin Exp Metastasis (2006) 23:19–31
DOI 10.1007/s10585-006-9008-z

ORIGINAL PAPER

The effect of zoledronic acid and osteoprotegerin on growth of human lung cancer in the tibias of nude mice

S. H. Tannehill-Gregg · A. L. Levine · M. V. P. Nadella · H. Iguchi · T. J. Rosol

Received: 12 April 2005 / Accepted: 22 March 2006 / Published online: 20 May 2006

Abstract The pathogenesis of bone metastases may require the activation of osteoclasts by tumor-secreted factors, which promote important interactions with the bone microenvironment. We utilized an intratibial model of bone metastasis with bioluminescent imaging (BLI) to measure the effect of osteoclast inhibition on the interaction of human lung cancer cells with bone, and on tumor growth. Mice were injected with luciferase-transduced tumor cells (HARA, human pulmonary squamous carcinoma) and divided into three groups: (1) untreated, (2) twice weekly treatment with the bisphosphonate zoledronic acid (ZOL), or (3) osteoprotegerin (OPG). Histomorphometry and imaging were used to evaluate tumor burden, and parameters of osteoclast activity. Mice in the treated groups had increased bone density and decreased osteoclast numbers in nontumor-bearing tibiae. There was greater than 60% reduction in mean tumor volume in both treatment groups when evaluated by histomorphometry ($P = 0.06$ [OPG], $P = 0.07$ [ZOL]). However, bioluminescent imaging failed to show a reduction in tumor burden due to wide variability in the data. Osteoclast numbers along tumor-associated bone were significantly increased compared to tumor-free bone, and were not reduced by either treatment. Plasma calcium concentration was increased in all groups. Plasma tartrate-resistant acid phosphatase 5b was reduced in both treatment groups. Plasma PTHrP was significantly increased in the untreated tumor-bearing group, but was not significantly different in the two treatment groups compared to normal mice. OPG or ZOL did not change tumor cell proliferation, but ZOL increased HARA cell apoptosis. OPG and ZOL reduced tumor growth in the tibiae of treated mice, however, PTHrP production by HARA cells may have resulted in a high concentration in the bone microenvironment, partially overriding the antiosteoclast effects of both OPG and ZOL.

Keywords Bioluminescent imaging · Bisphosphonate · Bone metastasis · Histomorphometry · Hypercalcemia · Mouse models · Osteoclast · Osteoprotegerin · Parathyroid hormone-related protein · Zoledronic acid

Abbreviations

BLI	bioluminescent imaging
IP	intraperitoneal
Luc	luciferase
OPG	osteoprotegerin
PTHrP	parathyroid hormone-related protein
SCC	squamous cell carcinoma
SQ	subcutaneous
TAB	tumor-associated bone
TRAcP	tartrate-resistant acid phosphatase
YFP	yellow-fluorescent protein
ZOL	zoledronic acid

Introduction

Metastases to bone cause significant morbidity and contribute to mortality in cancer patients. Death in association

S. H. Tannehill-Gregg
Bristol-Myers Squibb Company,
Pharmaceutical Research Institute,
Evansville, IN, USA

A. L. Levine · M. V. P. Nadella · T. J. Rosol (✉)
Department of Veterinary Biosciences, The Ohio State University, 307 Goss Laboratory, 1925 Coffey Road, Columbus, OH, USA
e-mail: rosol.1@osu.edu

H. Iguchi
Shikoku Cancer Center, Matsuyama, Japan

with cancer is more commonly due to complications from metastases rather than from the primary tumor [1]. Deleterious effects of bone metastases include bone pain, pathologic fracture, spinal cord compression, and the development of hypercalcemia [2]. Tumor-associated hypercalcemia can result in nausea, vomiting, dehydration, alteration of mental status, and renal failure [3].

Certain types of cancers more commonly metastasize to bone. Tumors originating in the breast, prostate or lung result in 80% of all bone metastases. Other types of cancers, such as gastrointestinal cancer, very rarely spread to bone [4]. The propensity of a certain type of cancer to spread to bone strongly supports the ''seed and soil'' hypothesis of Paget, namely that certain types of malignant cells (the 'seeds') are attracted to, and grow preferentially in, specific 'soils' (such as the bone microenvironment) [5]. Once the cells have implanted themselves in the bone microenvironment, their continued survival and growth is supported by the so-called 'vicious cycle of bone destruction'. This cycle is characterized by the production of various osteoclast-activating factors by the tumor cells (parathyroid hormone related protein [PTHrP], interleukins-1 and 6, tumor necrosis factor, and others). The activation of osteoclasts results in destruction of bone, releasing bone-associated growth factors (such as transforming growth factor-β, bone morphogenetic proteins, platelet-derived growth factors, fibroblast growth factors, and others), which in turn stimulate the tumor cells to proliferate and secrete more of the osteoclast-stimulating factors [3]. The cycle results in both tumor growth and increased destruction of bone, which contributes to hypercalcemia. The osteoclast plays a central role in the vicious cycle and makes an attractive therapeutic target.

There are several different mechanisms for cancer-associated hypercalcemia, including ectopic secretion of parathyroid hormone by tumor cells, tumor cell secretion of the active form of vitamin D, local osteolytic hypercalcemia, and humoral hypercalcemia of malignancy (HHM) [6]. In humoral hypercalcemia of malignancy (HHM) there is production of humoral factors [e.g., PTHrP] by tumor cells (in the primary tumor and its metastases) and secretion of the factors into the systemic circulation. In the case of PTHrP, hypercalcemia results from the stimulation of PTH1 receptors in both the kidney (increasing calcium reabsorption), and in bone (increasing osteoclastic bone resorption). In local osteolytic hypercalcemia, a large tumor burden in bone is associated with localized osteoclast activation and bone resorption, leading to the release of calcium into the systemic circulation [7].

The human lung squamous carcinoma cell line (HARA) used in this study represents a subtype of non-small cell lung cancer (NSLC) which has a propensity to metastasize to bone and is commonly associated with the production of PTHrP [7]. The normal keratinocyte both produces and secretes PTHrP, thus it is not surprising that squamous cell carcinomas are commonly associated with production of this polyhormone [8]. PTHrP is a major contributor to osteolytic (bone destructive) metastases due to its ability to indirectly activate osteoclasts through the PTH1 receptor on osteoblasts and stromal cells. This pathway involves the increased expression of RANKL (or 'osteoclast differentiation factor') on the osteoblast or stromal cells, which binds RANK on osteoclast precursors, resulting in osteoclast differentiation/maturation and activation. Osteoprotegerin (OPG) is a soluble decoy receptor for RANKL, and binding of RANKL to OPG results in the failure of RANK activation, and inhibition of osteoclast differentiation and activation [9]. The resorption of bone by mature osteoclasts results in the release and activation of bone-associated growth factors such as transforming growth factor-beta (TGF-β), which can act in a paracrine action on nearby tumor cells to upregulate the production of PTHrP by increasing mRNA stability [10].

The importance of PTHrP to the development and progression of bone metastases has been demonstrated in several rodent models of bone metastasis, including the MDA-MB-231 breast cancer mouse model. Treatment of mice with a monoclonal anti-PTHrP antibody after intracardiac injection of MDA-MB-231 cells resulted in a reduction in the formation of bone metastases and decreased bone destruction [11]. Rabbani et al. [12] demonstrated that overexpression of PTHrP in rat MatLyLu prostate cancer cells resulted in increased osteoclast activity in skeletal metastases in an intracardiac injection model.

Several treatments for cancer-associated hypercalcemia and metastases are currently available, including bisphosphonates [13, 14]. Bisphosphonates are inorganic pyrophosphate analogues which, upon administration, rapidly accumulate in bone and result in high levels in the bone microenvironment. Bisphosphonates are internalized by osteoclasts, and result in decreased bone resorption due to apoptosis of mature osteoclasts, suppression of osteoclastogenesis, and decreased function of mature osteoclasts [15]. More recently it has been demonstrated that nitrogen-containing bisphosphonates can have direct effects on neoplastic cells, including the induction of apoptosis, inhibition of migration (by decreasing matrix metalloproteases), and reduction in proliferation [16, 17]. Zoledronic acid is a nitrogen-containing third generation bisphosphonate which has demonstrated clinical efficacy in treating bone metastases and hypercalcemia in several types of solid cancer (including breast and non-small cell lung carcinoma) [18, 19].

The evaluation of osteoprotegerin for treatment of bone metastases is less well developed. Administration of OPG is expected to result in a local reduction in the RANKL/OPG ratio and inhibition of osteoclastic bone resorption.

Studies in mouse models of metastases have demonstrated decreased tumor burden and less bone destruction with OPG treatment using both breast and prostate cancer cells lines [20, 21].

We investigated whether treatment with zoledronic acid or OPG would decrease tumor burden and select plasma parameters of tumor burden and bone resorption by inhibiting osteoclastic bone resorption and tumor growth in an intratibial injection model of bone metastasis of a human pulmonary squamous cell carcinoma (HARA).

Materials and methods

Cell line

HARA, a cell line derived from a human pulmonary squamous cell carcinoma, was obtained from Dr. Haruo Iguchi, Shikoku Cancer Center, Matsuyama, Japan. The original human patient had increased serum parathyroid hormone-related protein (PTHrP) concentration and hypercalcemia, but no apparent bone metastases. The cell line expresses and secretes PTHrP, and mice given intracardiac injections of HARA cells develop bone metastases [22]. Cells were maintained in RPMI 1640 (Invitrogen Co., Carlsbad, CA) supplemented with 10% fetal bovine serum, 250 units/ml penicillin, and 250 μg/ml streptomycin (Invitrogen Co.) in a humidified 37°C incubator with 5% CO_2.

Generation of lentiviral vectors and HARA transduction

A 2,183 bp Luciferase/Yellow Fluorescent Protein fusion construct flanked by *SfuI* and *XhoI* was PCR amplified from pCDNA3.1(+).yLuc-YFP (obtained from Dr. Christopher Contag, Stanford University, Stanford, CA) and subcloned into pCR4TOPO (Invitrogen Co., Carlsbad, CA), excised, and gel purified. The Luc/YFP construct was cloned into a retroviral vector, pHIVSIN-Luc (obtained from Dr. Kathleen Boris-Lawrie, The Ohio State University, Columbus, OH), replacing a 1,491 bp Luc fragment in the plasmid. The new plasmid was named pHIVSIN-Luc/YFP. Lentiviral vectors were produced by transient triple transfection of 293T cells (obtained from Dr. Michael Lairmore, The Ohio State University, Columbus, OH) in DMEM (Invitrogen Co., Carlsbad, CA) with 10% FBS using calcium phosphate (Sigma–Aldrich Co., St. Louis, MO) and 10 μg of packaging plasmid pCMVΔR8.2, 2 μg of envelope plasmid pMD.G (both obtained from Dr. Kathleen Boris-Lawrie) and pHIVSIN-Luc/YFP. The vector particles in the supernatant were filtered through a 0.2 μm filter and sedimented by ultracentrifugation at 6,500×*g* for 16 h at 4°C. The pellets were redissolved in DMEM resulting in a 1,000-fold concentration. HARA cells (in RPMI with 10% FBS) were transduced with polybrene (8 μg/ml) (Sigma–Aldrich Co., St. Louis, MO) and the virus by spin-inoculation at 2,700 rpm for 1 h at 32°C (HARA-YFP/Luc).

Mice, tumor inoculation

Male nu/nu mice were purchased from the Charles River Laboratories (Wilmington, MA). Mice were housed in microisolator cages, and were provided food pellets and water ad libitum. Mice were anesthetized with 3.5 mg ketamine/0.15 mg xylazine intraperitoneally (IP), and 50,000 HARA-YFP/Luc cells were suspended in 10 μl sterile Dulbeccos's PBS and injected through the skin into the proximal left tibia using the tibial crest as a landmark. Injections were performed using a 25-gauge needle and a 100 μl Hamilton syringe (Hamilton Co., Reno, NV). Mice were imaged on day one post-injection, then weekly for 4 weeks.

Treatments

Mice were divided into three groups of 20 mice each. One group was injected with HARA cells and did not receive osteoprotegerin or zoledronic acid. The other two groups of mice were treated twice weekly for 4 weeks with recombinant human Fc-osteoprotegerin, 50 μg/mouse, IP (Amgen, Thousand Oaks, CA) or zoledronic acid, 0.625 μg/mouse, subcutaneously (SQ) (Novartis, Basel, Switzerland). The first dose was administered the day before tumor cell injection. Twice weekly injections of vehicle in untreated mice were not performed. Weekly bioluminescent imaging (involving intraperitoneal injections of luciferin and anesthesia with box induction; details below) was performed on all mice and equalized the levels of stress experienced by each group.

Imaging

In vivo bioluminescent imaging was performed on a cooled CCD IVIS™ system equipped with a 50 mm lens (Xenogen Corp., Alameda, CA). Results were analyzed using LivingImage® software, version 2.2 (Xenogen Corp.). Mice received IP injections of D-luciferin (Xenogen Corp.), 4.3 mg/mouse, dissolved in sterile PBS. The exact time of luciferin injection was recorded. Mice were anesthetized with 3% isoflurane/induction in a box system and 1.5% isoflurane/maintenance via a nose cone delivery system. Oxygen was delivered at 1L/min. Body temperature was maintained throughout imaging using a 37°C platform in

the chamber. Lateral images of five mice were acquired simultaneously at several set time points extending to a maximum of 20 min after luciferin injection (Fig. 1). Integration times and binning varied depending on the saturation level of the group of mice being imaged. Times ranged from 10 s to 1 min, binning was small (4) or medium (8), and the f/stop used was 1. Field of view (FOV) was maintained at position C (20 cm). Pseudo-color images of photon emissions were overlaid on grayscale images of animals to aid in fixing spatial distribution of signals. Photon quantitations were calculated within regions of interest (ROIs) overlying the left tibias, as well as a background determination from a signal-free region of the mouse. Tumor burden at day 30 was determined by dividing photons/s emission at day 30 by that from day 1. This allowed normalization of data for the actual numbers of cells initially injected.

Histopathology

Mice were sacrificed at 30 days post-injection, blood was collected and plasma was separated using heparinized Microtainer® tubes (Becton Dickinson, Franklin Lakes, NJ) and stored at −80°C. Legs were separated at the coxofemoral joint, defleshed and fixed in 10% neutral-buffered formalin for 24 h at 4°C. Legs were decalcified in 10% EDTA, pH 7.4 at 4°C for 2–3 weeks. Decalcified tibias and lungs were embedded in paraffin, cut into 5 μm sections, mounted on slides, and stained with hematoxylin and eosin. Freshly cut sections of the tibias were also stained for osteoclasts utilizing tartrate-resistant acid phosphatase enzyme histochemistry as described by van der Pluijm et al. [23]. Briefly, 5 μm paraffin sections were rehydrated and incubated with substrate solution for 30 min containing naphthol AS-BI phosphate as substrate dissolved in Michelis veronal acetate buffer, hexazonium pararosaniline as a coupler, and 10 mM of L(+)tartaric acid as an inhibitor (Sigma–Aldrich Co., St. Louis, MO). Slides were counterstained with hematoxylin. Histomorphometry was performed using the Bioquant Nova image analysis system (Bioquant Image Analysis Corp., Nashville, TN). Trabecular area of metaphyseal bone was measured in one 200 mm^2 window in each tibia. Osteoclast parameters (perimeter and number) were measured in two windows in each tibia (400 mm^2 total). Tumor area was measured in four sections from each tibia. Osteoclast numbers and perimeter were measured along tumor-associated bone by evaluating one section from each tibia.

Plasma calcium concentration

Calcium concentration was measured using 10 μl of plasma and a colorimetric assay performed on a dry chemistry analyzer (VITROS DT60; Ortho-Clinical Diagnostics, Rochester, NY). Ten nontumor-bearing age- and sex-matched nude mice were used as controls for normal plasma calcium concentrations.

Plasma PTHrP concentration

Plasma PTHrP (1–86) concentration was measured using a two-site immunoradiometric assay (Diagnostic Systems Laboratories, Inc., Webster, TX). Radioactivity was measured using a gamma scintillation counter for 1 min. Results were calculated using a log–log curve fit, then converted to pmol/L by multiplying pg/ml by 0.101. Four nontumor-bearing age- and sex-matched nude mice were used as controls for normal plasma PTHrP concentrations.

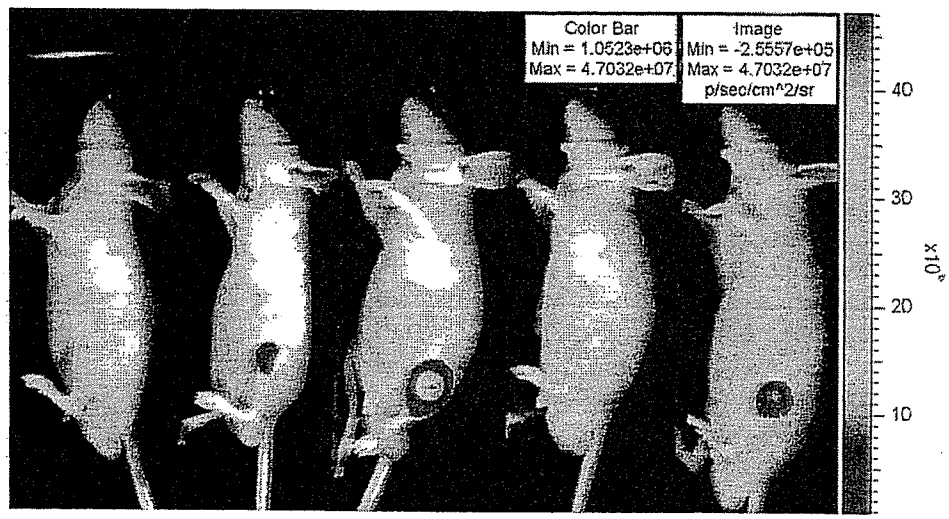

Fig. 1 Bioluminescent imaging of mice from the osteoprotegerin-treated group. Thirty days post-HARA injection, after intraperitoneal injection of luciferin. A region of interest was used to analyze the photons emitted/second from a specified area. The highest level of photon emission corresponded to the orange/red end of the color spectrum. The fourth mouse was injected with cells; photon emission was present but very low. Note the wide variability in tumor growth in the mice

Plasma TRAcP 5b activity

Tartrate-resistant acid phosphatase 5b activity specific to mouse osteoclasts was measured using a solid phase immunofixed-enzyme activity assay (MouseTRAP Assay) (Immunodiagnostic Systems, Inc., Fountain Hills, AZ). Absorbencies were measured at 405 nm wavelength on an UVmax Kinetic Microplate Reader (Molecular Devices, Sunnyvale, CA).

Ki67 Immunohistochemistry

Ki-67 immunohistochemistry of tumors was performed at The Ohio State University Hospitals, Department of Surgical Pathology. Three 400× fields were evaluated for each tumor. Proliferation rate was estimated by dividing the number of positive tumor cells by the number of total tumor cells counted in the three fields. The average number of cancer cells counted per mouse was 1,100.

TUNEL Staining

Apoptosis was detected utilizing the TdT-FragEL™ DNA fragmentation detection kit (Calbiochem, San Diego, CA). The staining procedures were performed based on the manufacturers' recommendations. Briefly, after deparaffinization, rehydration and washing in 1× TBS, tissues were digested with proteinase K (20 μg/ml) for 20 min at room temperature and washed. Endogenous peroxidases were blocked with 3% H_2O_2 and slides were incubated with equilibration buffer. Sections were treated with terminal deoxynucleotidyltransferase (TdT) enzyme for 90 min in a humidified chamber at 37°C. After histochemical staining with peroxidase streptavidin and diaminobenzidine, slides were counterstained with methyl green, dehydrated and cover slipped. Control slides were included with the kit and consisted of HL-60 cells incubated with 0.5 μg/ml actinomycin D for 19 h to induce apoptosis and uninduced HL-60 cells. A negative control was generated by omitting TdT. For each section evaluated, the total area of tumor (μm^2) was calculated using BioQuant Nova image analysis system (Bioquant Image Analysis Corp., Nashville, TN). The total number of apoptotic neoplastic cells was counted for each section and results were expressed as the number of apoptotic cells per area of tumor.

Exclusion of data

Mice were removed from all analyses if it was determined by histology that the initial injection of cells was not directly into the tibia (most commonly into surrounding muscle). This resulted in the removal of one mouse from the untreated group, two mice from the OPG-treated group, and three mice from the zoledronic acid-treated group.

Statistical analysis

Statistical analysis of data was performed using Sigmastat 3.2 (Systat Software, Inc., Richmond, CA). A one-way ANOVA was used to compare normally distributed data. A Kruskal–Wallis one-way analysis of variance on ranks was used to compare data that was not normally distributed. Secondary tests included Dunn's and Holm-Sidak Methods. Incidence of lung metastases were analyzed by Chi Square Independent testing and Fisher's Exact Test.

Results

Trabecular area and osteoclast measurements of non-injected (right) tibia (Fig. 2)

Evaluation of the non-injected (right) leg was used to confirm the biological effect of drug administration. Trabecular area of metaphyseal bone was significantly increased in both treatment groups when compared to untreated mice (Fig. 3a). Osteoclast perimeter (the percentage of metaphyseal trabecular perimeter lined by osteoclasts) and osteoclast number (per mm of trabecular bone) were significantly decreased in both treatment groups when compared to untreated mice (Fig. 3b, c). The significant increase in trabecular area (due to continued bone growth but decreased osteoclastic bone resorption), and decrease in osteoclast measurements in metaphyseal bone were expected after treatment with antiosteoclast agents. These results indicated that the dose and route of administration of zoledronic acid and OPG were sufficient to result in the appropriate physiologic effect in normal metaphyseal bone.

Tumor burden

The mean tumor areas in the OPG and zoledronic acid-treated groups were reduced by 62% and 67%, respectively ($P = 0.06$ for OPG, $P = 0.07$ for zoledronic acid), when evaluated by histomorphometry (Fig. 4a). The data did not fit a normal distribution. The mean tumor volumes between groups as evaluated by bioluminescent IVIS imaging were reduced by 14% (OPG) and 43.4% (zoledronic acid) (Fig. 4b). The data did not fit a normal distribution and there was no significant difference from controls ($P = 0.60$).

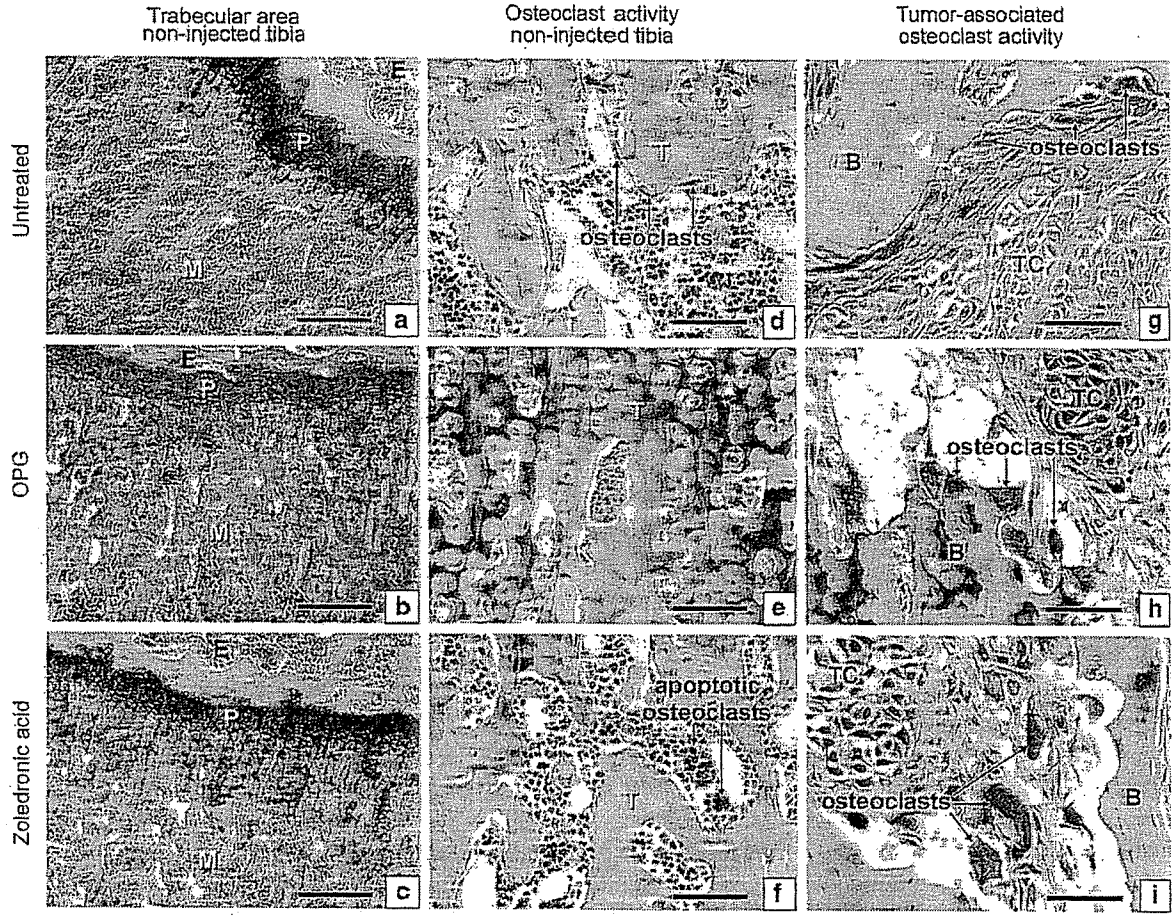

Fig. 2 Representative tibias from non-injected and injected mice. Panels **a–c** (non-injected leg) illustrate the marked increase in trabecular area in the osteoprotegerin (OPG) (**b**) and zoledronic acid (**c**)-treated mice when compared to the untreated group. Panels **d–f** (non-injected leg) illustrate the marked decrease in osteoclast perimeter and number in the OPG (**e**) and zoledronic acid (**f**)-treated mice when compared to the untreated group. Panels **g–i** (injected leg) illustrate the increased number of osteoclasts along tumor-associated bone in all three groups. Panels **a–c**: magnification = 100×, Bar = 300 μm. Panels **d–i**: magnification = 400×, Bar = 75 μm. All sections stained for tartrate-resistant acid phosphatase with hematoxylin counterstain. (P = physis; E = epiphysis; M = metaphysis; T = trabeculae; B = bone; TC = tumor cells)

Osteoclast measurements along tumor-associated bone (Fig. 2)

Osteoclast activity was significantly increased along tumor-associated bone (TAB) when compared to trabecular bone in non-injected legs in all groups. There was no significant difference in osteoclast perimeter (Fig. 5a) or numbers (Fig. 5b) along TAB between the untreated group and either of the treatment groups.

Incidence of tumor growth in lung

One mouse of nineteen in the untreated group, one mouse of seventeen in the zoledronic acid-treated group, and four mice of eighteen in the OPG-treated group developed small foci of tumor growth in the lung. The incidence of tumor growth in the lung did not differ significantly between groups (Chi Square Independent testing ($P = 0.17$) and Fisher's Exact Test ($P = 0.30$)).

Plasma calcium concentration

Plasma calcium concentrations were significantly increased in all three groups ($P < 0.05$) when compared to normal nontumor-bearing mice, however there was no significant difference in plasma calcium between the three tumor-bearing groups (Fig. 6a).

Plasma PTHrP concentration

Plasma PTHrP concentration was significantly increased in the tumor-bearing untreated mice compared to normal

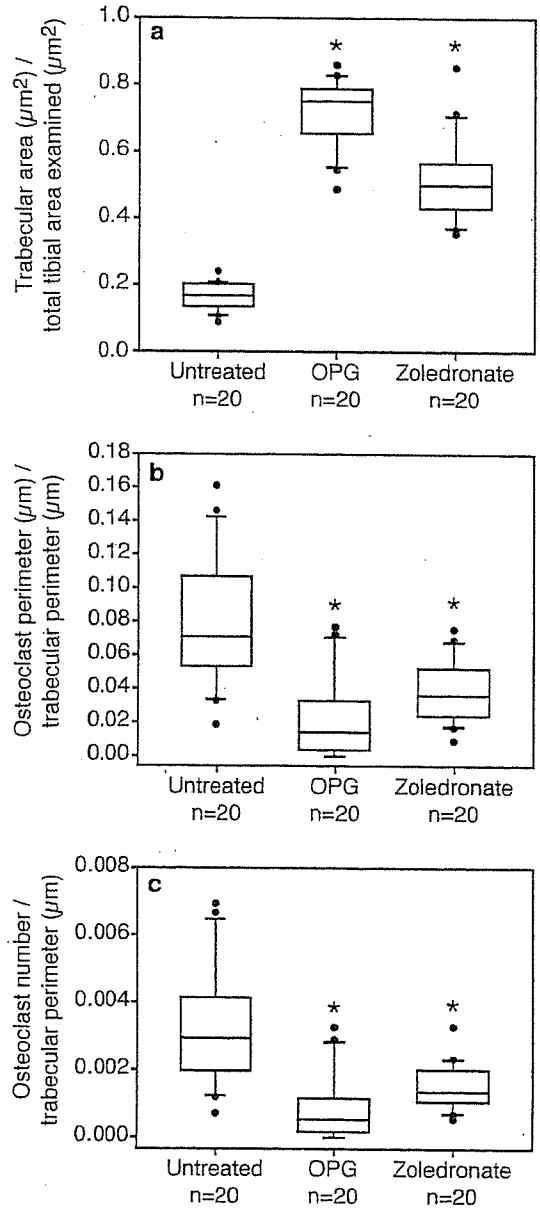

Fig. 3 Trabecular area and osteoclast measurements, non-injected tibias. Trabecular area (**a**) was significantly increased in both treatment groups when compared to untreated mice (*$P < 0.001$). The area was calculated from a 200 μm^2 field in the metaphysis. Osteoclast perimeter (**b**) and number (**c**) were significantly decreased in both treatment groups when compared to untreated mice (*$P < 0.001$ for both). Osteoclast measurements were calculated from two 200 μm^2 fields in the metaphysis. (**a–c**) Boxes represent quartiles and the whiskers represent the 10th and 90th percentiles. Outliers are represented as separate points. OPG = osteoprotegerin. Zoledronate = zoledronic acid

nontumor-bearing mice (Fig. 6b). This is likely due to production and secretion of PTHrP by the HARA cells in vivo. Plasma PTHrP in the zoledronic acid-treated group was significantly decreased compared to the tumor-bearing untreated mice. Plasma PTHrP levels in the OPG-treated mice were not significantly different from tumor-bearing untreated mice. Zoledronic acid appeared to have a greater effect on reduction in plasma PTHrP levels than OPG (Fig. 6b).

Plasma TRAcP 5b

Plasma TRAcP 5b is present in high levels in osteoclasts, is secreted into the systemic circulation, and is a specific, sensitive marker of bone resorption [24]. Inhibition of osteoclasts is expected to result in decreased plasma TRAcP 5b concentration. Plasma TRAcP 5b was significantly decreased in both treatment groups when compared to the untreated group (Fig. 6c). This was interpreted to reflect an overall net decrease in osteoclast activity throughout the mouse in response to both treatments. The increased osteoclast numbers along tumor-associated bone were felt to represent a local phenomenon, which did not contribute appreciably to increasing circulating TRAcP 5b levels.

Ki67 immunohistochemistry

The tumor cells in all three groups had a high level of immunostaining for Ki67, a marker of cell proliferation. Positive staining of HARA cells in the untreated group was $69 \pm 2\%$ (mean ± SEM) ($n = 11$), in the OPG group was $72 \pm 4\%$ (mean ± SEM) ($n = 7$), and in the zoledronic acid group was $62 \pm 4\%$ (mean ± SEM) ($n = 8$). Treatment with OPG ($P = 0.233$) or zoledronic acid ($P = 0.097$) did not statistically significantly alter Ki67 immunostaining as compared to the untreated group.

TUNEL assay

The rate of apoptosis of the HARA cells in the untreated group was 1.4×10^{-2} cells/mm^2 ($n = 10$), in the OPG group was 1.0×10^{-2} cells/mm^2 ($n = 6$) and in the zoledronic acid group was 3.5×10^{-2} cells/mm^2 ($n = 5$). Although OPG did not induce apoptosis, mice treated with ZOL had a modest increase in tumor cell apoptosis ($P = 0.068$).

Discussion

The marked propensity of some types of cancer to metastasize specifically to bone and the significant contributions to cancer-associated morbidity and mortality that bone metastases make has resulted in an intense search for methods to prevent and treat this manifestation of cancer. The bone pain, pathologic fractures, and hypercalcemia that can be associated with bone metastases have been

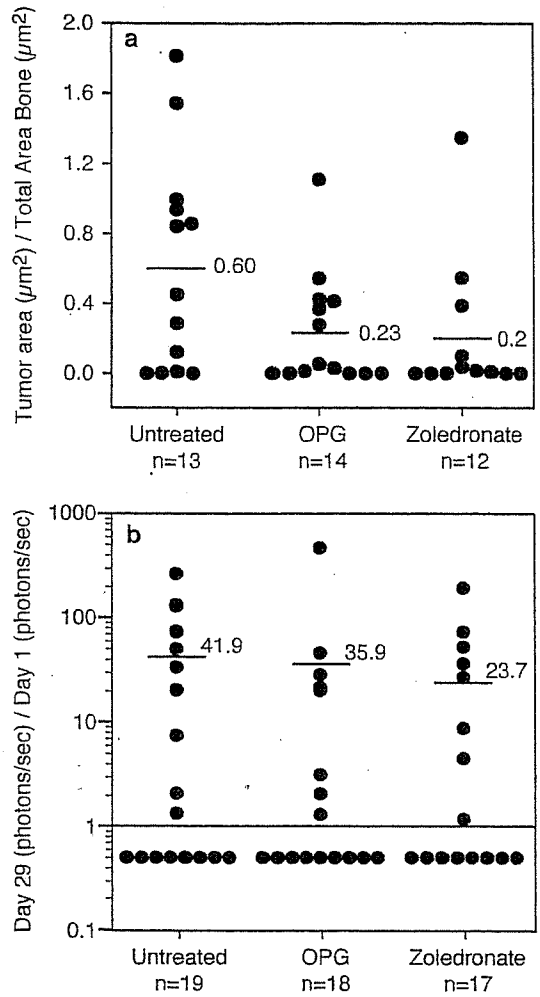

Fig. 4 Tumor burden. (**a**) Histomorphometrical analysis. There was a marked reduction in the mean tumor burden by 62% (OPG) and 67% (zoledronic acid) in treated mice compared to the untreated group; variability in the data precluded attaining statistical significance. The horizontal bars and adjacent numbers represent group means. Values represent the percent of tibial area occupied by tumor. Four sections from each mouse were analyzed. (**b**) In vivo bioluminescent imaging analysis. There was a reduction in the mean tumor burden by 14% (OPG) and 43% (zoledronic acid) compared to the untreated group; variability in the data precluded attaining statistical significance. Variability was greater than the analysis of tumor burden by histomorphometry. Data represents a ratio of photon/second emission on day 29 to that on day 1 to control for the actual number of cells injected into each tibia. Data points <1 are not represented in calculated values. The horizontal bars and adjacent numbers represent group means. OPG = osteoprotegerin. Zoledronate = zoledronic acid

treated with varying success by using chemotherapy, hormonal therapy, irradiation, surgery, and more recently by agents such as bisphosphonates, which have antiosteoclast and antitumor activity [3].

Bisphosphonates are currently used in the treatment of established bone metastases. Trials with zoledronic acid have demonstrated a delay in skeletal events in patients with breast cancer metastatic to bone [25] and non-small cell lung carcinoma [19], and zoledronic acid has proven benefit in prostate cancer [26].

The use of osteoprotegerin (OPG) for the treatment of bone metastases is less well-established. Animal models have demonstrated that treatment with OPG reduces the growth of both prostate carcinoma and breast cancer in bone [20, 21, 27]. A human trial using OPG has been published (in patients with osteolytic breast carcinoma or multiple myeloma). OPG treatment resulted in suppression of bone resorption as measured by urinary *N*-telopeptide of collagen/creatinine and was well tolerated [28].

Metastasis to bone involves numerous steps starting with the initial detachment of neoplastic cells from the primary tumor mass, invasion through surrounding connective tissue to blood vessels, travel through the blood with evasion of immune detection, and arrest and growth in the secondary site [29]. The intratibial model of bone metastasis represents the final step of the metastatic cascade, namely the survival and proliferation of neoplastic cells in the bone microenvironment. In our intratibial injection model, preventive treatment (treatment started prior to tumor cell injection) with zoledronic acid or osteoprotegerin showed a marked reduction of tumor burden in mice when analyzed by histomorphometry. Analysis of tumor burden using in vivo bioluminescent imaging resulted in a higher degree of variability in the data and was less sensitive than histomorphometry, since the amount of bioluminescence did not always correlate to tumor size as visualized grossly and measured using histopathological sections. Standard histomorphometry, with evaluation of four sections from each tumor-bearing tibia, was interpreted to have resulted in a more accurate quantification of tumor burden.

Others have demonstrated that in vivo bioluminescent imaging (BLI) can be a useful technique to estimate tumor burden [30, 31]. The advantages of such a system include the ability to serially analyze response to treatment and tumor growth without euthanasia of animals, the use of fewer animals in each experiment, and the ability to analyze the volume of viable tumor tissue since light emission from the entire tumor is measured, compared to the traditional two-dimensional area measurements used by standard histomorphometry. However, there are challenges with quantitation of viable tumor tissue by BLI as demonstrated by our study. In this investigation, and using this transduced cell line, histomorphometry was more accurate than BLI at measuring tumor volume and emphasizes the need to confirm BLI data with morphometry. This was likely due to the unexpected wide variability in the BLI data. We controlled for variable injection volumes by dividing day 30 data by that from day 1. BLI is a very sensitive technique that is useful to

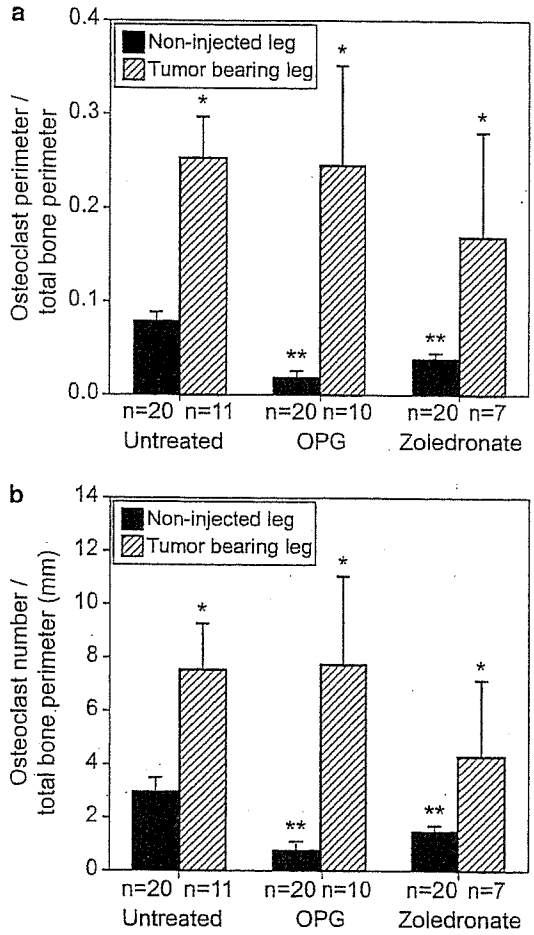

Fig. 5 Osteoclast measurements along tumor-associated bone. Osteoclast perimeter (**a**) and number (**b**) along tumor-associated bone were significantly increased compared to the non-injected (tumor-free) leg (*$P < 0.05$), and treatment with either osteoprotegerin (OPG) or zoledronic acid (zoledronate) did not significantly reduce osteoclast measurements along tumor-associated bone. Treatments significantly decreased osteoclast perimeter (**a**) and number (**b**) in the non-injected (tumor-free) legs (**$P < 0.001$). The bars represent the mean of each group, with the standard error mean indicated by the whisker.

identify small numbers of tumor cells at metastatic sites; however, variability in tumor activity or expression of luciferase can lead to a wide variation in the in vivo data. To obtain an accurate representation of tumor volume using BLI, the neoplastic cells must be actively expressing luciferase at the time of imaging. Loss of expression of the construct (in all or subsets of the tumor cells), areas of necrosis within the tumor, or variable luciferase expression by tumor cells would result in inaccurate representation of tumor volume. While the tumors in our model did not have large areas of necrosis, it is possible that loss or variable expression of the luciferase construct contributed to the variability in tumor burden when measured by this method.

The HARA human pulmonary squamous cell carcinoma line produces and secretes high levels of the potent osteoclast-activating factor, parathyroid hormone-related protein (PTHrP) [22]. We hypothesize that production of PTHrP by the tumor cells resulted in a high localized concentration of PTHrP in the bone microenvironment, at least partially overriding the antiosteoclast effect of either OPG or zoledronic acid. The production of PTHrP would explain not only the increased osteoclasts along tumor-associated bone (TAB) in the untreated animals, but also the lack of reduction in osteoclast perimeter and number along TAB in both treatment groups. We have recently reported that PTHrP mRNA was increased in HARA cells up to 20-fold in bone metastases in mice compared to subcutaneous tumors (Deng et al. (2006) Cancer Res in review). In contrast, the nontumor bearing leg in treated mice showed the expected response to OPG or zoledronic acid treatment (reduction in osteoclast measurements and increase in trabecular area).

In other models of bone metastasis using PTHrP-producing cell lines (PC-3, MDA-231, LNCaP) and treatment with OPG or zoledronic acid, investigators reported significantly reduced tumor burden and osteoclasts along TAB, however doses, routes of administration (subcutaneous versus intravenous), initiation of treatment (preventive versus treatment mode), and cell type (breast versus lung versus prostate) varied, making it difficult to directly compare results from other studies [20, 21, 32]. For OPG, doses ranged from 2 mg/kg to 25 mg/kg and treatment frequency from twice a week to three times a week. Although the dose and frequency of administration of OPG used in this experiment was at the lower end of those used in other experiments, the marked reduction in osteoclast number and perimeter in the non-injected tibiae in our model demonstrated that levels of OPG were high enough to have a physiologic effect in normal tibias. It is possible that the antiosteoclast effect was not attained in the injected tibias as a result of tumor-induced changes, such as localized disruption of blood flow or high local concentrations of osteoclast-stimulating factors, such as PTHrP. The dose of zoledronic acid used in this experiment (0.025 mg/kg) was lower than that used in other animal

►

Fig. 6 Plasma parameters. (**a**) Plasma calcium concentration was significantly increased in all three treatment groups compared to normal mice ($P < 0.05$). Treatment with either drug did not significantly decrease plasma calcium concentration. (**b**) Plasma PTHrP was significantly increased above the nontumor-bearing mice ("normal") in the untreated group (*$P < 0.05$). Plasma PTHrP in the zoledronic acid group (but not the OPG group) was significantly decreased below that of the untreated group (**$P < 0.05$). (c) Plasma TRAcP 5b was significantly decreased (*$P < 0.05$) in both treatment groups when compared to the untreated mice. The limit of detection for this assay was 0.1 U/L. All horizontal bars indicate the group means. OPG = osteoprotegerin. Zoledronate = zoledronic acid

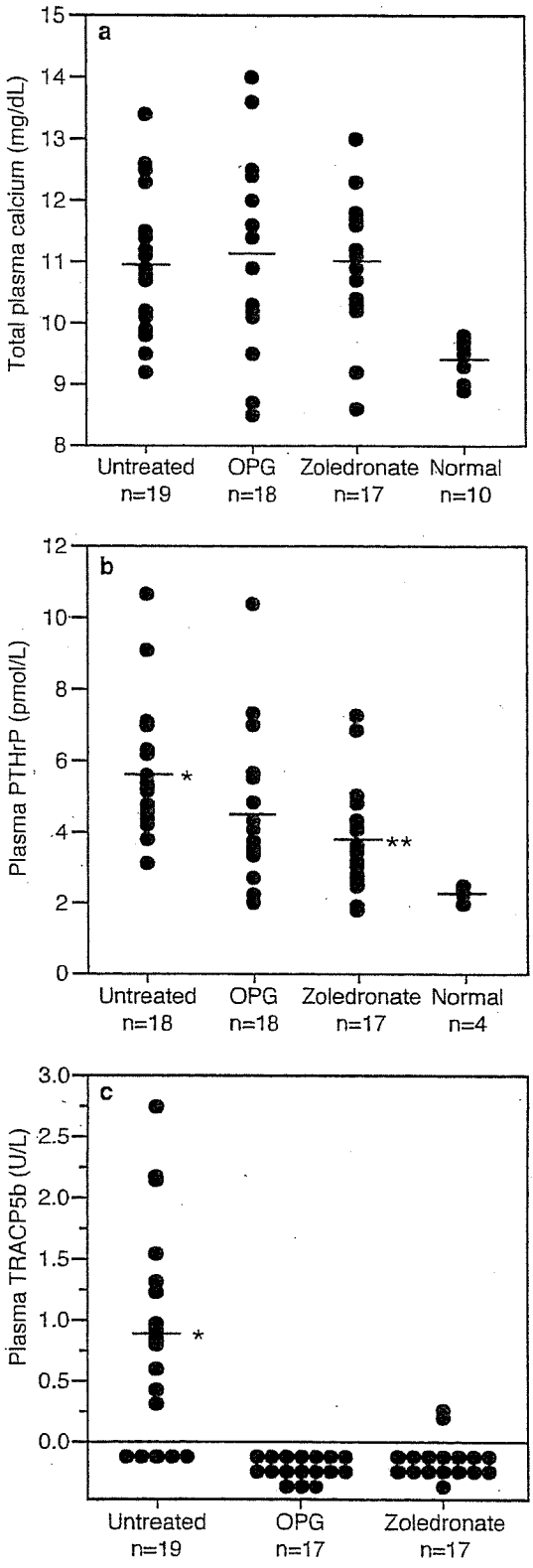

models of bone metastasis. For example, in an intratibial prostate carcinoma model, Corey et al. [32] used 0.2 mg/kg. Based on allometric scaling, which takes into account inherent differences in metabolic activity between different species, our dose is more than 10× lower than that typically used clinically in humans [33]. However, in our experiments, zoledronic acid was administered twice weekly, which is more frequent than the current clinical use in humans (where it is typically administered as a 4 mg intravenous infusion once every 3–4 weeks) [34]. Despite the dose used, the decreased numbers of osteoclasts and increased trabecular bone observed in the nontumor-bearing tibial metaphyses indicated a physiologic effect in normal bone. As with OPG, it is possible that disruption of the normal blood flow to the metaphyses in the tumor-bearing legs (due to the presence of the tumor) affected the ability of the drug to reach this region, or that increased local levels of a pro-osteoclast agent, such as PTHrP, antagonized the effects of the zoledronic acid. We would predict that using higher doses of either drug, or inhibiting PTHrP production by the HARA cells, would result in a greater reduction in tumor burden and a reduction in osteoclastic bone resorption along tumor-associated bone.

Bisphosphonates are the treatment of choice for cancer-induced hypercalcemia due to their antiosteoclast activity [35]. OPG has been used to reduce cancer-associated hypercalcemia in several mouse models [36, 37]. In our study, mice in all three groups had significant increases in plasma calcium compared to normal mice, with no reduction in plasma calcium concentration by treatment with zoledronic acid or OPG. We hypothesize that OPG and zoledronic acid were unable to block the effects of locally high levels of PTHrP in the immediate vicinity of the tumor leading to osteoclast activation along TAB and hypercalcemia in the mice. The untreated mice also likely had a humoral contribution from increased plasma concentrations of PTHrP.

Nitrogen-containing bisphosphonates have been reported to decrease the proliferation rate and increase apoptosis of cancer cells [38, 39]. In contrast, PTHrP has been reported to increase the proliferation rate of cancer cells [40], and to protect against apoptosis in breast cancer cells [41]. Osteoprotegerin has been reported to be an anti-apoptotic survival factor through its binding of tumor necrosis factor-related apoptosis-inducing ligand (TRAIL) [42, 43], as well as to have no effect on apoptosis in vitro [21]. The HARA cells in the zoledronic acid-treated group had a mild increase in apoptosis. Increased PTHrP in the bone microenvironment due to secretion from HARA cells may have interfered with the ability of zoledronic acid and OPG to significantly alter the proliferation rate and level of apoptosis of the HARA cells.

In vitro studies that have demonstrated antiproliferative and pro-apoptotic effects of bisphosphonates used high concentrations of the drugs, ranging from 5 to 2,000 μM [17]. Bisphosphonates concentrate in bone by avid binding to hydroxyapatite, which likely leads to high concentrations of the drugs in the bone microenvironment [34]. However, bisphosphonates are not metabolized and are cleared rapidly from the plasma [15]; peak plasma levels after intravenous infusion of zoledronic acid are reported to be in the 1–2 μM range, far lower than that used in in vitro experiments [J. Green, personal communication]. It is uncertain whether the high concentrations used in cytostatic in vitro studies accurately reflect what occurs in the bone microenvironment in the in vivo setting [34]. Osteoprotegerin has not been shown to have a cytostatic effect on cancer cells in vitro [21]. In our study, the similar reduction in tumor burden using both zoledronic acid and osteoprotegerin supports the concept that the effects on tumor burden were indirect. In other words, the reduction was likely related to the antiosteoclast effect of each drug, rather than a cytostatic effect.

The prevention of bone metastases by bisphosphonates is less well established than their use for the treatment of bone metastases. Human clinical trials and animal models have had mixed results. Two human clinical trials using clodronate for the prevention of skeletal metastases in patients with early stage-breast cancer had contrasting results. One trial had a survival benefit, and one trial had decreased survival. Trials using the more potent zoledronic acid in a preventive manner are planned [34]. Animal models of bone metastasis prevention using bisphosphonates have also yielded contrasting results as well as interesting information on the role of bisphosphonates in the development of soft tissue metastases. In such animal models some studies demonstrated a decrease in bone metastases but an increase in soft tissue metastases [44]. Other studies have demonstrated a decrease in bone metastases and no effect on soft tissue metastases [45]. While others demonstrated a decrease in soft tissue metastases [46]. The variation in results likely reflects, at least partially, the administration of different bisphosphonates by different routes and doses, and the use of different tumor cell types and routes of tumor cell inoculation in these models. The variable results with regard to the effect of bisphosphonates on soft tissue tumor growth and metastasis make the use of such drugs in patients without clinical evidence of bone metastases (in a 'preventive' capacity) potentially riskier [34, 47]. In our intratibial injection model of lung cancer preventive treatment with zoledronic acid demonstrated no difference in the growth of tumor cells in the lungs in spite of a reduction in tibial tumor burden, but lung metastasis was an infrequent finding in this investigation.

The effect of OPG treatment on the development of visceral metastases has not been investigated as thoroughly as it has been for bisphosphonates. Morony et al. [20] demonstrated that administration of OPG at the time of tumor cell injection had no effect on the development of visceral metastases, and Zhang et al. [21] found that OPG had no effect on subcutaneous growth of prostate cancer when administered at the time of tumor cell injection. Despite the lack of an effect on the growth of neoplastic cells in soft tissue, both experiments demonstrated a marked decrease in skeletal growth of neoplastic cells with OPG treatment. Similarly, in our intratibial injection model of lung cancer, the use of OPG in a preventive manner did not result in any difference in the growth of metastatic tumor cells in the lung, despite reducing tumor burden in injected tibias.

In conclusion, we utilized an intratibial model of a luciferase-expressing human pulmonary squamous cell carcinoma line (HARA) to investigate the effects of treatment with the antiosteoclast agents zoledronic acid and osteoprotegerin. There was a marked reduction in tumor burden with both treatments when analyzed by histomorphometry. The lack of a decrease in osteoclasts along tumor-associated bone was likely due to the production of high levels of PTHrP or other cytokines antagonizing the antiosteoclast effects of zoledronic acid or OPG that were evident on bone surfaces in the nontumor-bearing tibia. Further evaluation of this model using HARA cells with reduced PTHrP production could clarify the role of PTHrP in the bone microenvironment.

Acknowledgements We would like to acknowledge Jeff Pan and Soledad Fernandez for statistical assistance, Tim Vojt for preparation of figures, Ann Saulsbery and Alan Flechtner for histotechnology support, University laboratory animal resources staff for animal care assistance, and Guangchun He and Drs. Gwendolyn Lorch, Ramiro Toribio, Alex Luchin, Nanda Thudi, Xiyun Deng, Jun Liu for laboratory support. Dr. Toribio also assisted with the statistical analysis. This work was supported by the National Institutes of Health, National Cancer Institute (K08 CA83766 for STG and R01 CA77911 for TJR) and the National Center for Research Resources (K26 RR00168 and S10 RR17841 for TJR).

References

1. Jemal A, Thomas A, Murray T et al (2002) Cancer statistics, 2002. CA Cancer J Clin 52:23–47
2. Tu SM, Lin SH (2004) Clinical aspects of bone metastases in prostate cancer. In: Keller ET, Chung LWK (eds) The biology of skeletal metastases, 1st edn. Kluwer Academic Publishers, Boston, pp 23–46
3. Guise TA, Mundy GR (1998) Cancer and bone. Endocr Rev 19:18–54
4. Galasko CSB (1986) Incidence and distribution of skeletal metastases. In: Galasko CSB (ed) Skeletal metastases, 1st edn. Butterworths, London, pp 14–21

5. Paget S (1989) The distribution of secondary growths in cancer of the breast. 1889. Cancer Metastasis Rev 8:98–101
6. Stewart AF (2005) Hypercalcemia associated with cancer. N Engl J Med 352:373–379
7. Morton AR, Lipton A (1995) Hypercalcemia. In: Abeloff MD, Armitage JO, Lichter AS et al (eds) Clinical oncology, 1st edn. Churchill Livingstone, New York, pp 527–542
8. Weckmann MT, Grone A, Capen CC et al (1997) Regulation of parathyroid hormone-related protein secretion and mRNA expression in normal human keratinocytes and a squamous carcinoma cell line. Exp Cell Res 232:79–89
9. Wittrant Y, Theoleyre S, Chipoy C et al (2004) RANKL/RANK/OPG: new therapeutic targets in bone tumours and associated osteolysis. Biochim Biophys Acta 1704:49–57
10. Sellers RS, Capen CC, Rosol TJ (2002) Messenger RNA stability of parathyroid hormone-related protein regulated by transforming growth factor-beta1. Mol Cell Endocrinol 188:37–46
11. Guise TA, Yin JJ, Taylor SD et al (1996) Evidence for a causal role of parathyroid hormone-related protein in the pathogenesis of human breast cancer-mediated osteolysis. J Clin Invest 98:1544–1549
12. Rabbani SA, Gladu J, Harakidas P et al (1999) Over-production of parathyroid hormone-related peptide results in increased osteolytic skeletal metastasis by prostate cancer cells in vivo. Int J Cancer 80:257–264
13. Perry CM, Figgitt DP (2004) Zoledronic acid: a review of its use in patients with advanced cancer. Drugs 64:1197–1211
14. Rosen LS (2004) New generation of bisphosphonates: broad clinical utility in breast and prostate cancer. Oncology (Huntingt) 18:26–32
15. Ramaswamy B, Shapiro CL (2003) Bisphosphonates in the prevention and treatment of bone metastases. Oncology (Huntingt) 17:1261–1270
16. Boissier S, Ferreras M, Peyruchaud O et al (2000) Bisphosphonates inhibit breast and prostate carcinoma cell invasion, an early event in the formation of bone metastases. Cancer Res 60:2949–2954
17. Green JR (2003) Antitumor effects of bisphosphonates. Cancer 97:840–847
18. Cameron D (2003) Proven efficacy of zoledronic acid in the treatment of bone metastases in patients with breast cancer and other malignancies. Breast 12(Suppl 2):S22–S29
19. Rosen LS, Gordon D, Tchekmedyian NS et al (2004) Long-term efficacy and safety of zoledronic acid in the treatment of skeletal metastases in patients with nonsmall cell lung carcinoma and other solid tumors: a randomized, Phase III, double-blind, placebo-controlled trial. Cancer 100:2613–2621
20. Morony S, Capparelli C, Sarosi I et al (2001) Osteoprotegerin inhibits osteolysis and decreases skeletal tumor burden in syngeneic and nude mouse models of experimental bone metastasis. Cancer Res 61:4432–4436
21. Zhang J, Dai J, Qi Y et al (2001) Osteoprotegerin inhibits prostate cancer-induced osteoclastogenesis and prevents prostate tumor growth in the bone. J Clin Invest 107:1235–1244
22. Iguchi H, Tanaka S, Ozawa Y et al (1996) An experimental model of bone metastasis by human lung cancer cells: the role of parathyroid hormone-related protein in bone metastasis. Cancer Res 56:4040–4043
23. van der Pluijm G, Most W, van der Wee-Pals L et al (1991) Two distinct effects of recombinant human tumor necrosis factor-alpha on osteoclast development and subsequent resorption of mineralized matrix. Endocrinology 129:1596–1604
24. Halleen JM (2003) Tartrate-resistant acid phosphatase 5B is a specific and sensitive marker of bone resorption. Anticancer Res 23:1027–1029
25. Lipton A (2003) Bisphosphonates and metastatic breast carcinoma. Cancer 97:848–853
26. Eaton CL, Coleman RE (2003) Pathophysiology of bone metastases from prostate cancer and the role of bisphosphonates in treatment. Cancer Treat Rev 29:189–198
27. Yonou H, Kanomata N, Goya M et al (2003) Osteoprotegerin/osteoclastogenesis inhibitory factor decreases human prostate cancer burden in human adult bone implanted into nonobese diabetic/severe combined immunodeficient mice. Cancer Res 63:2096–2102
28. Body JJ, Greipp P, Coleman RE et al (2003) A phase I study of AMGN-0007, a recombinant osteoprotegerin construct, in patients with multiple myeloma or breast carcinoma related bone metastases. Cancer 97:887–892
29. Robinson VL, Kauffman EC, Sokoloff MH et al (2004) The basic biology of metastasis. Cancer Treat Res 118:1–21
30. Edinger M, Cao YA, Hornig YS et al (2002) Advancing animal models of neoplasia through in vivo bioluminescence imaging. Eur J Cancer 38:2128–2136
31. Kalikin LM, Schneider A, Thakur MA et al (2003) In vivo visualization of metastatic prostate cancer and quantitation of disease progression in immunocompromised mice. Cancer Biol Ther 2:656–660
32. Corey E, Brown LG, Quinn JE et al (2003) Zoledronic acid exhibits inhibitory effects on osteoblastic and osteolytic metastases of prostate cancer. Clin Cancer Res 9:295–306
33. Freireich EJ, Gehan EA, Rall DP et al (1966) Quantitative comparison of toxicity of anticancer agents in mouse, rat, hamster, dog, monkey, and man. Cancer Chemother Rep 50:219–244
34. Brown JE, Neville-Webbe H, Coleman RE (2004) The role of bisphosphonates in breast and prostate cancers. Endocr Relat Cancer 11:207–224
35. Saunders Y, Ross JR, Broadley KE et al (2004) Systematic review of bisphosphonates for hypercalcaemia of malignancy. Palliat Med 18:418–431
36. Akatsu T, Murakami T, Ono K et al (1998) Osteoclastogenesis inhibitory factor exhibits hypocalcemic effects in normal mice and in hypercalcemic nude mice carrying tumors associated with humoral hypercalcemia of malignancy. Bone 23:495–498
37. Capparelli C, Kostenuik PJ, Morony S et al (2000) Osteoprotegerin prevents and reverses hypercalcemia in a murine model of humoral hypercalcemia of malignancy. Cancer Res 60:783–787
38. Forsea AM, Muller C, Riebeling C et al (2004) Nitrogen-containing bisphosphonates inhibit cell cycle progression in human melanoma cells. Br J Cancer 91:803–810
39. Green JR, Clezardin P (2002) Mechanisms of bisphosphonate effects on osteoclasts, tumor cell growth, and metastasis. Am J Clin Oncol 25:S3–S9
40. Falzon M, Du P (2000) Enhanced growth of MCF-7 breast cancer cells overexpressing parathyroid hormone-related peptide. Endocrinology 141:1882–1892
41. Tovar SV, Shen X, Falzon M (2002) Intracrine PTHrP protects against serum starvation-induced apoptosis and regulates the cell cycle in MCF-7 breast cancer cells. Endocrinology 143:596–606
42. Holen I, Croucher PI, Hamdy FC et al (2002) Osteoprotegerin (OPG) is a survival factor for human prostate cancer cells. Cancer Res 62:1619–1623
43. Neville-Webbe HL, Cross NA, Eaton CL et al (2004) Osteoprotegerin (OPG) produced by bone marrow stromal cells protects breast cancer cells from TRAIL-induced apoptosis. Breast Cancer Res Treat 86:269–279
44. Yoneda T, Michigami T, Yi B et al (2000) Actions of bisphosphonate on bone metastasis in animal models of breast carcinoma. Cancer 88:2979–2988

45. Michigami T, Hiraga T, Williams PJ et al (2002) The effect of the bisphosphonate ibandronate on breast cancer metastasis to visceral organs. Breast Cancer Res Treat 75:249–258
46. Hiraga T, Williams PJ, Ueda A et al (2004) Zoledronic acid inhibits visceral metastases in the 4T1/luc mouse breast cancer model. Clin Cancer Res 10:4559–4567
47. Hillner BE, Ingle JN, Berenson JR et al (2000) American Society of Clinical Oncology guideline on the role of bisphosphonates in breast cancer. American Society of Clinical Oncology Bisphosphonates Expert Panel. J Clin Oncol 18:1378–1391

J Bone Miner Metab (2006) 24:16–19
DOI 10.1007/s00774-005-0640-5

ORIGINAL ARTICLE

Haruo Iguchi · Yuko Aramaki · Shigeaki Maruta
Soichi Takiguchi

Effects of anti-parathyroid hormone-related protein monoclonal antibody and osteoprotegerin on PTHrP-producing tumor-induced cachexia in nude mice

Received: February 21, 2005 / Accepted: August 2, 2005

Abstract We have previously demonstrated that parathyroid hormone-related protein (PTHrP) is a cachexia inducer, but it is still not known what PTHrP effects on target tissues induce the cachexia. Therefore, we examined the effects of anti-PTHrP antibody and osteoprotegerin (OPG) on PTHrP-producing tumor-induced cachexia. Nude mice bearing PTHrP-producing human lung cancer cells (HARA-B) exhibited cachexia with hypercalcemia 3–4 weeks after inoculation, accompanied by losses in body, adipose tissue, and muscle weight. OPG ameliorated hypercalcemia, as did neutralization of PTHrP with antibody; and it increased both body and adipose tissue weights. These increases in body and adipose tissue weight, however, were significantly less than those in mice treated with anti-PTHrP antibody. Simultaneous administration of OPG and anti-PTHrP antibody caused significant increases in body, adipose tissue, and muscle weight, along with an immediate decrease in blood ionized calcium levels. The increase in body weight was similar to that observed in mice treated with anti-PTHrP antibody alone, and the decrease in the blood ionized calcium levels was significantly greater than that in mice treated with OPG or anti-PTHrP antibody alone. These results suggest that an effect of PTHrP on target tissues other than hypercalcemia is involved in the development of cachexia. Expression of cachexia-inducing proinflammatory cytokines (interleukin-6 and leukemia inhibitory factor) is stimulated by PTHrP. This might be a mechanism by which PTHrP produces tumor-induced cachexia. It is also suggested that OPG and anti-PTHrP antibody synergistically act to ameliorate hypercalcemia, although the mechanism responsible for this is unclear.

H. Iguchi (✉) · Y. Aramaki · S. Maruta · S. Takiguchi
Division of Tumor Dynamics, National Kyushu Cancer Center, 3-1-1 Notame, Minami-ku, Fukuoka 811-1395, Japan
Tel. +81-92-541-3231; Fax +81-92-551-4585
e-mail: higuchi@nk-cc.go.jp

Key words PTHrP · cachexia · hypercalcemia · osteoprotegerin · anti-PTHrP antibody

Introduction

Cachexia is a debilitating condition of involuntary weight loss characterized by anorexia, depletion of fat and muscle tissues, hypoglycemia, and anemia [1]. It often accompanies various cancers in advanced stages and reduces the quality of life and the patient's response to chemotherapy [2]. For cachexic patients, the normal balance between energy intake and caloric expenditure is disrupted owing to increased catabolism. However, the molecular mechanism responsible for cachexia is poorly understood. Several cytokines, including tumor necrosis factor-α (TNFα [3]) interleukin-6 (IL-6) [4]) interferon-γ [5], and leukemia inhibitory factor ((LIF) [6]) have been implicated in the development of cancer cachexia; and recently we showed that parathyroid hormone-related protein (PTHrP) induces cachexia in experimental animals using cultured human lung cancer cells [7]. In this cachexia model, however, it remains unclear what PTHrP effects on target tissues induce cachexia.

Osteoprotegerin (OPG) is a member of the tumor necrosis factor receptor family and antagonizes the ability of receptor activator of nuclear factor κ-B ligand (RANKL) to bind to its receptor, the receptor activator of nuclear factor κ-B (RANK) [8,9]. OPG prevents and reverses hypercalcemia in an animal model of humoral hypercalcemia of malignancy (HHM) [10], and the effect of OPG on hypercalcemia occurs via the competitive inhibition of RANKL–RANK interaction regardless of the action of PTHrP. Thus, to determine the role of PTHrP in cachexia, we examined the effects of OPG on cachexia in an experimental cachexia model induced by a PTHrP-producing tumor and compared its effects to those of anti-PTHrP monoclonal antibody (mAb).

Materials and methods

HARA-B cachexia model

HARA-B cells were isolated from a bone metastasis of human lung cancer-derived cells (HARA), which induces cachexia with hypercalcemia [7]. The cells were cultured in RPMI-1640 plus 10% fetal bovine serum (FBS) and penicillin-streptomycin, harvested by trypsinization, and resuspended in phosphate-buffered saline (PBS). A single suspension of HARA-B cells (5×10^6 cells/0.2ml) were inoculated subcutaneously (s.c.) in the right flank of nude mice (5-week-old male mice).

Administration of anti-PTHrP antibody and OPG

Anti-human PTHrP mAb was provided by Chugai Pharmaceutical Japan; the characteristics of this mAb were previously described [11]. The recombinant OPG used was provided by Amgen and comprised the ligand-binding domain of human OPG fused to the Fc domain of human immunoglobulin G (IgG) [8].

HARA-B-bearing mice began losing body weight 3–4 weeks after inoculation. Tumor weight was estimated by the formula ($ab^2/2$), and the carcass weight was calculated as the difference between the whole-body weight and the estimated tumor weight. The followings were administered when the carcass weight fell to below 20g: anti-human PTHrP mAb (100μg IgG/mouse, intraperitoneal (i.p.) infusion on day 0); OPG (2.5mg/kg s.c. infusion on days 0–5); anti-human PTHrP mAb (100μg IgG/mouse i.p. infusion on day 0) + OPG (2.5mg/kg s.c. infusion on days 0–5); and PBS (0.1ml/mouse i.p. on day 0).

Body weight and tumor size were measured daily. Blood ionized calcium levels in retroorbital samples were measured on days 0, 2, 4, and 6 by the electrode method using an autoanalyzer (M-634; Chiba Corning Diagnostics, Toyko, Japan). Mice were killed on day 6 after administration of these agents. At this time blood was collected from the heart; and the epididymal adipose tissue, gastrocnemius muscle, and subcutaneous tumor were weighed. Serum samples obtained after centrifugation were stored at –30°C until serum PTHrP levels were determined. Serum PTHrP levels were measured using a radioimmunoassay (RIA) kit specific for the C-terminal portion of PTHrP (Daiichi, Toyko, Japan).

Statistics

Statistical analysis was performed using Welch's unpaired *t*-test. $P < 0.05$ indicated statistical significance.

Results

HARA-B-bearing mice exhibited a reduction in body weight 3–4 weeks after inoculation. The effects of anti-PTHrP mAb, OPG, and anti-PTHrP mAb plus OPG were examined in mice whose body weight dropped below 20g. The changes in body weight and blood ionized calcium levels are shown in Fig. 1. Administration of anti-PTHrP mAb or OPG caused weight gain, and the body weights of mice treated with anti-PTHrP mAb or OPG were significantly higher than those of the control mice over the observation period. However, the increase in body weight of mice treated with anti-PTHrP mAb was greater than that of mice treated with OPG, and the differences between them were significant from days 2 to 6 after administration. The blood ionized calcium levels of mice treated with anti-PTHrP mAb immediately decreased and remained at levels similar to those of mice treated with OPG. Blood ionized calcium levels in these groups were

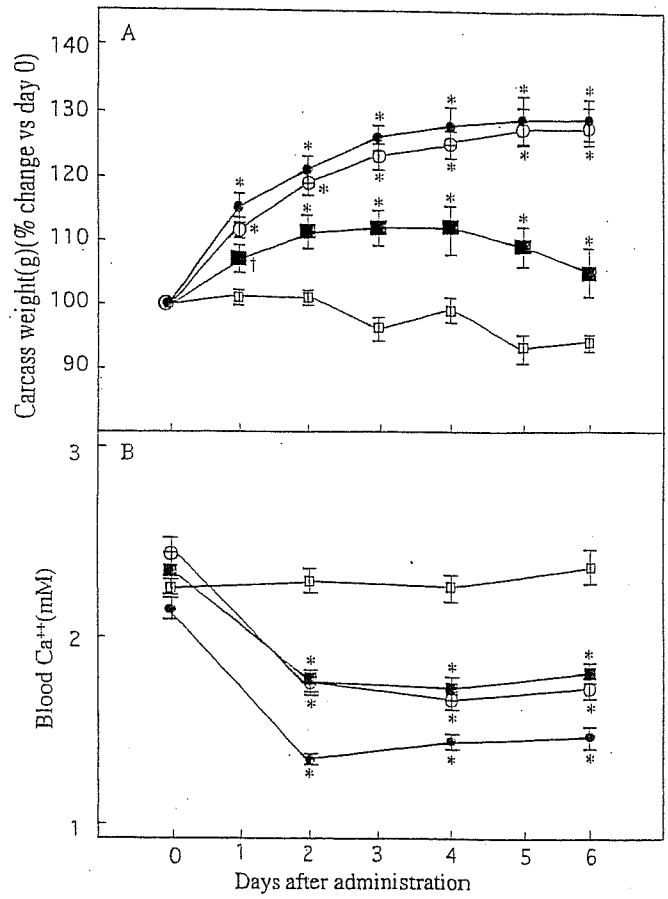

Fig. 1. Changes in body (carcass) weight (**A**) and blood ionized calcium levels (**B**) in HARA-B-bearing mice after administration of phosphate-buffered saline (control) (*open square*), osteoprotegerin (OPG) (*filled squares*), anti-parathyroid hormone-related protein (anti-PTHrP) monoclonal antibody (mAb) (*open circles*) and OPG plus anti-PTHrP mAb (*filled circles*). When the carcass weight fell below 20g, PBS and anti-PTHrP mAb (100μg immunoglobulin G) were administered to the peritoneal cavity on day 0, and OPG (2.5mg/kg) was administered subcutaneously from days 0 to 5. The body weight and tumor size were measured daily, and blood ionized calcium was measured on days 0, 2, 4, and 6. The mice were sacrificed on day 6 after administration. The carcass weight was calculated as the difference between the whole-body weight and the estimated tumor weight. The values represent means for groups of eight mice. *Vertical bars* are the SE. $^*P < 0.001$. $^\dagger P < 0.05$

Table 1. Cachexia parameters of HARA-B-bearing mice and age-matched non-tumor-bearing mice (normal) after various treatments

Parameter	HARA-B-bearing mice				Normal mice
	Controls	Antibody	OPG	Antibody + OPG	
Carcass weight (g)	17.0 ± 0.4	23.4 ± 0.5*	20.4 ± 0.6*	24.0 ± 0.6*	27.0 ± 0.7
Adipose tissue weight (mg)	18 ± 4.1	108 ± 9.2*	58 ± 11*	120 ± 9.2*	81 ± 9.4
Muscle weight (mg)	89 ± 2.4	108 ± 4.2*	94 ± 3.7	108 ± 2.2*	125 ± 2.8
Tumor weight (g)	2.9 ± 0.3	2.5 ± 0.3	2.3 ± 0.2	2.7 ± 0.3	
Blood Ca^{2+} (mM)	2.36 ± 0.09	1.72 ± 0.05*	1.80 ± 0.05*	1.46 ± 0.06*	1.34 ± 0.01
Serum PTHrP (pmol/l)	1102 ± 119	905 ± 82	1192 ± 159	1130 ± 198	59 ± 10

* $P < 0.001$ vs control

Data are expressed as the mean ± SE from eight mice treated with PBS (controls), anti-PTHrP mAb (Antibody), OPG, and anti-PTHrP mAb plus OPG (Antibody + OPG) and six non-tumor-bearing mice (Normal)

PBS, phosphate-buffered saline; PTHrP, parathyroid hormone-related protein; mAb, monoclonal antibody; OPG, osteoprotegerin

significantly lower than those of the controls on days 2, 4, and 6 after administration.

We also examined the combined effects of anti-PTHrP mAb plus OPG on HARA-B-bearing mice. Simultaneous administration of anti-PTHrP mAb plus OPG caused weight gain, and the change in body weight was similar to that of mice treated with anti-PTHrP mAb. Blood ionized calcium levels decreased to a greater extent than those of mice treated with anti-PTHrP mAb or OPG, and significant differences in the blood ionized calcium levels were found on days 2, 4, and 6 after administration.

Losses in adipose tissue weight and muscle weight usually develop in cachexic mice. HARA-B-bearing mice showed marked depletion of adipose tissue weight and mild depletion of muscle weight [7]. Several cachexia parameters measured on day 6 after administration are shown in Table 1. Treatment with anti-PTHrP mAb caused a significant increase in adipose tissue weight and muscle weight. Treatment with OPG also increased adipose tissue weight, but it was significantly less than that of mice treated with anti-PTHrP mAb. Simultaneous treatment with anti-PTHrP mAb plus OPG resulted in a significant increase in adipose tissue and muscle weights compared to the controls, which was similar to that of mice treated with anti-PTHrP mAb. There were no significant differences between the tumor weights or serum PTHrP levels among groups.

Discussion

We previously reported that PTHrP induces cancer cachexia in an experimental model using human lung cancer-derived cells [7]. However, it remains to be determined what PTHrP effects on target tissues induce cachexia. We therefore examined the effects of OPG, which inhibits hypercalcemia, on PTHrP-producing tumor-induced cachexia to elucidate the mechanism responsible for this condition. OPG inhibited hypercalcemia to the same extent as that caused by neutralization of PTHrP with antibody. OPG also increased the body and adipose tissue weights compared with the controls, although these effects were less when compared to those in mice treated with the neutralization of PTHrP with antibody. In addition, OPG failed to cause an increase in the muscle weight.

These results suggest that hypercalcemia is involved in the development of PTHrP-producing tumor-induced cachexia, but that its contribution is limited. The conditions responsible for cachexia cannot be explained by anorexia and energy expenditure, as nutritional support is unable to alleviate this syndrome [12]. Mechanisms other than anorexia could be involved in the induction of cachexia. The direct effects of cytokines may be involved in the loss of adipose tissue and muscle weights. IL-6 suppresses the expression of lipoprotein lipase, a key enzyme that regulates lipid metabolism in adipocytes during cachexia [13]. In the present study, the loss in adipose tissue and muscle weights were fully recovered, not by correcting the hypercalcemia but by neutralizing PTHrP with antibody. This raises the possibility that PTHrP causes the catabolism of adipose tissue and muscle through a mechanism other than hypercalcemia. PTHrP plays another role as a proinflammatory cytokine and stimulates the expression of IL-6 and LIF, which are both known as cachexia inducers, through the cytokine cascade [14]. In our previous study, however, serum levels of mouse IL-6 in HARA-B-bearing mice with cachexia were similar to those in the non-tumor-bearing mice [7]. We cannot exclude the possibility that PTHrP may act through the endogenous release of these cachexia-inducing proinflammatory cytokines (IL-6 and LIF) only at the target sites in a paracrine fashion, which would not influence the serum levels of these cytokines.

PTHrP is expressed in discrete regions of the brain [15]. We therefore cannot exclude the possibility that PTHrP induces anorexia by altering central neurohormonal signals that govern appetite. However, food intake was only minimally decreased due to HARA-B-induced cachexia in a previous study [7], suggesting that anorexia is not involved in this cachexia.

OPG was identified as an osteoclastogenesis inhibitory factor (OCIF) that inhibits osteoclast formation and activity [8,9]; and several studies have found that OPG inhibits bone resorption caused by several cytokines including PTHrP [16]. Furthermore, Capparelli et al. [10] showed that OPG prevents and reverses hypercalcemia in an HHM model mouse. In the present study, the hypercalcemia in HARA-

B-bearing mice was ameliorated by OPG, anti-PTHrP mAb, or both. The blood ionized calcium levels were decreased to a greater extent after simultaneous administration of OPG and anti-PTHrP mAb compared to those after OPG or anti-PTHrP mAb alone. OPG together with anti-PTHrP mAb almost completely normalized the hypercalcemia. Although the mechanism responsible for the synergistic effects of OPG and anti-PTHrP mAb on hypercalcemia is not clear, hypercalcemia in the HARA-B-bearing mice may be induced not only by PTHrP but also by other factors, and further studies are required to elucidate the mechanism for the development of hypercalcemia in HARA-B-bearing mice.

In conclusion, PTHrP is a known mediator of cachexia. Hypercalcemia, which is induced by PTHrP, as well as other effects of PTHrP (partly through the induction of cachexia-inducing proinflammatory cytokines at the target sites) cooperate to develop cachexia. In addition, OPG and anti-PTHrP antibody additively inhibit hypercalcemia.

Acknowledgments This study was supported in part by Health and Labor Science Research Grants: Research on Human Genome, Tissue Engineering Food Biotechnology (H15-Genome-002) and by a Grant-in-Aid for Cancer Research (14–16) from the Ministry of Health, Labor, and Welfare, Japan.

References

1. Tisdale MJ (2001) Cancer anorexia and cachexia. Nutrition 17:438–442
2. Dewys WD, Begg C, Lavin PT, Band PR, Bennett JM, Bertino JR (1980) Prognostic effect of weight loss prior to chemotherapy in cancer patients. Am J Med 69:491–497
3. Oliff A, Defeo-Jones D, Boyer M, Martinez D, Kiefer D, Vuocolo G, Wolfe A, Socher SH (1987) Tumor secreting human TNF/cachectin induce cachexia in mice. 50:555–563
4. Strassman G, Fong M, Kenney JS, Jacob CO (1992) Evidence for the involvement of interleukin 6 in experimental cancer cachexia. J Clin Invest 89:1681–1684
5. Matthys P, Dijkmans R, Proost P, Van Damme J, Heremans H, Sobis H, Billiau A (1991) Severe cachexia in mice inoculated with interferon-γ-producing tumor cells. Int J Cancer 49:77–82
6. Mori M, Yamaguchi K, Honda S, Nagasaki K, Ueda M, Abe O, Abe K (1991) Cancer cachexia syndrome developed in nude mice bearing melanoma cells producing leukemia-inhibitory factor. Cancer Res 51:6656–6659
7. Iguchi H, Onuma E, Sato K, Sato K, Ogata E (2001) Involvement of parathyroid hormone-related protein in experimental cachexia induced by a human lung cancer-derived cell line established from a bone metastasis specimen. Int J Cancer 94:24–27
8. Simonet WS, Lacey DL, Dunstan CR, Kelley M, Chang MS, et al. (1997) Osteoprotegerin: a novel secreted protein involved in the regulation of bone density. Cell 89:309–319
9. Tsuda E, Goto M, Mochizuki S, Yano K, Kobayashi F, Morinaga T, Higashio K (1997) Isolation of a novel cytokine from human fibroblasts that specifically inhibits osteoclastogenesis. Biochem Biophys Res Commun 234:137–142
10. Capparelli C, Kostenuik PJ, Morony S, Starnes C, Weimann B, Van G, Scully S, Qi M, Lacey DL, Dunstan CR (2000) Osteoprotegerin prevents and reverses hypercalcemia in a murine model of humoral hypercalcemia of malignancy. Cancer Res 60: 783–787
11. Sato K, Yamakawa Y, Shizume K, Satoh T, Nohotomi K, Demura H, Akatsu T, Nagata N, Kasahara T, Ohkawa H (1993) Passive immunization with anti-parathyroid hormone-related protein monoclonal antibody markedly prolongs survival time of hypercalcemic nude mice bearing transplanted human PTHrP-producing tumors. J Bone Miner Res 8:849–860
12. Kotler DP (2000) Cachexia. Ann Intern Med 133:622–634
13. Greenberg AS, Nordan RP, McIntosh J, Calvo JC, Scow RO, Jablons D (1992) Interleukin 6 reduces lipoprotein lipase activities in adipose tissue of mice in vivo and in 3T3-L1 adipocytes: a possible role for interleukin 6 in cancer cachexia. Cancer Res 52:4113–4116
14. Pollock JH, Blaha MJ, Lavish SA, Stevenson S, Greenfield E (1996) In vivo demonstration that parathyroid hormone and parathyroid hormone-related protein stimulate expression by osteoblasts of interleukin-6 and leukemia inhibitory factor. J Bone Miner Res 11:754–759
15. Wier EC, Brines ML, Ikeda K, Burtis WJ, Broadus AE, Robbins RJ (1990) Parathyroid hormone-related peptide gene is expressed in the mammalian central nervous system. Proc Natl Acad Sci USA 87:108–112
16. Morony S, Capparelli C, Lee R, Shimamoto G, Boone T, Lacey DL, Dunstan CR (1999) Osteoprotegerin inhibits hypercalcemia and increased bone resorption induced by IL-Iβ, TNF-α, PTH, PTHrP, and 1,25-dihydroxyvitamin D_3. J Bone Miner Res 14:1478–1485

Characteristic features of disseminated carcinomatosis of the bone marrow due to gastric cancer: The pathogenesis of bone destruction

HIROKI KUSUMOTO[1], MASARU HARAGUCHI[1], YOKO NOZUKA[2], YOSHINAO ODA[2], MASAZUMI TSUNEYOSHI[2] and HARUO IGUCHI[3,4]

[1]Division of Gastroenterological Surgery, National Kyushu Cancer Center; [2]Department of Anatomical Pathology, Faculty of Medicine, Kyushu University; [3]Division of Tumor Dynamics, National Kyushu Cancer Center Research Institute, Fukuoka, Japan

Received March 31, 2006; Accepted June 19, 2006

Abstract. Disseminated carcinimatosis of the bone marrow is accompanied by solid tumors, and gastric cancer accounts for the majority. The prognosis of this condition is poor, however, the pathogenesis for wide-spread bone lesions has yet to be elucidated. In 9 patients with gastric cancer demonstrating disseminated carcinomatosis of the bone marrow, the characteristic clinicopathological features were examined. Immunohistochemistry for receptor activator of NF-κB ligand (RANKL) and parathyroid hormone-related protein was also performed on gastric cancer tissue and bone marrow specimens to identify the factors responsible for the occurrence of bone lesions in patients presenting with this condition. The characteristic features of disseminated carcinomatosis of the bone marrow due to gastric cancer include a yonger patient age, an elevation of serum alkaline phosphatase and/or lactate dehydrogenase levels, wide-spread bone metastases with osteolytic bone destruction, a low incidence of hypercalcemia and a histological gastric cancer type of either signet ring cell carcinoma or poorly diffentiated adenocarcinoma. The expression of RANKL, which is one of the master regulators of osteoclastic bone resorption in bone metastasis, was also found in gastric cancer cells obtained from such patients. The RANKL expressed in gastric cancer may therefore play a critical role in the promotion of osteoclast formation, which has been suggested to be involved in the pathogenesis of bone lesions.

Correspondence to: Dr Haruo Iguchi, [4]*Present address*: Shikoku Cancer Center, Minamiumemotomachi Ko 160, Matsuyama, Japan
E-mail: higuchi@shikoku-cc.go.jp

Key words: gastric cancer, bone marrow invasion, bone destruction, receptor activator of NF-κB ligand

Introduction

Bone metastases diffusely invading the bone marrow with hematological disorders [i.e., disseminated intravascular coagulation (DIC), microangiopathic hemolytic anemia, etc.] tend to be accompanied by solid tumors (1), and this condition is called disseminated carcinomatosis of the bone marrow. This condition is often caused by gastric cancer among solid tumors, although its overall incidence is rare (2,3). The prognosis for this condition is extremely poor, however, the pathogenesis of this condition, namely the cause for the development of such diffuse bone metastases, has yet to be elucidated. In the present study, we examined the characteristic clinicopathological features of disseminated carcinomatosis of the bone marrow accompanied by gastric cancer based on the clinical findings of 9 cases who presented with this condition at our cancer center from 1991 to 2002. We also examined the expression of receptor activator of NF-κB ligand (RANKL) and parathyroid hormone-related protein (PTHrP), which are known to be master regulators of osteoclastic bone resorption in bone metastasis (4,5), in gastric cancer tissue and bone marrow specimens obtained from these 9 patients to identify any factors related to the pathogenesis of such diffuse bone metastases observed in this condition.

Patients and methods

Patients. Nine patients with disseminated carcinomatosis of the bone marrow associated with gastric cancer, who were treated in our cancer center between 1991-2002, were examined.

The diagnosis of disseminated carcinomatosis of the bone marrow was made in patients with gastric cancer, who also demonstrated: i) an elevation of the serum alkaline phosphatase (ALP) and/or lactate dehydrogenase (LDH) levels, ii) DIC and/or anemia (macro- to normocytic and hyper- to normochromic anemia), and iii) diffuse bone metastases on the bone scintigraphy findings. A bone marrow puncture was performed on 2 patients (cases 5 and 9 in Table I), and metastatic infiltration of atypical epithelial cells (cancer cells) was found in a bone marrow aspiration smear (Fig. 1). Eight

Table I. Clinicopathological features of nine patients with disseminated carcinomatosis of the bone marrow associated with gastric cancer.

Case	Age (years)	Sex	ALP[a] (IU/l)	LDH[a] (IU/l)	Hematological disorders[b] DIC	Hematological disorders[b] Anemia	Hypercalcemia[c]	Histological type[d]	Therapy[e]	Survival period (days)[f]	Immunohistochemistry RANKL	Immunohistochemistry PTHrP	Type of bone metastasis
1	52	F	475	584	+	+	-	Sig	CDDP/5-FU	100	-	-	Osteolytic
2	40	F	395	1179	+	+	-	Mo	BSC	58	+	-	Osteolytic
3	49	F	1188	310	+	+	-	Sig	CDDP/5-FU	240	+	+	Osteolytic
4	45	M	892	4820	+	+	+	Po	BSC	43	+	-	Osteolytic
5	65	M	234	1915	-	+	-	Sig	BSC	10	+	-	NE
6	63	M	1336	1380	+	+	-	Sig	MTX/5-FU	190	-	+	NE
7	50	M	168	432	-	+	-	Mo	BSC	110	+	-	NE
8	63	M	668	465	-	+	+	Po	MTX/5-FU	220	-	+	Osteolytic
9	40	F	2404	1720	+	-	-	Mo	MTX/5-FU BP	330	+	-	Osteolytic

[a]Serum levels of alkaline phosphatase (ALP) (normal 45-130 IU/l) and lactate dehydrogenase (LDH) (normal 200-370 IU/l) at diagnosis. [b]Associated hematological disorders at diagnosis. [c]Incidence of hypercalcemia during the course of the disease. [d]Histological types of primary gastric cancer. Sig, signet ring cell carcinoma; Po, poorly differentiated adenocarcinoma; Mo, moderately differentiated adenocarcinoma. [e]CDDP, cisplatinum; 5-FU, 5-fluorouracil; MTX, methotrexate; BP, bisphosphonates; BSC, best supportive care. [f]Survival period since the diagnosis of disseminated carcinomatosis of the bone marrow. NE, not examined.

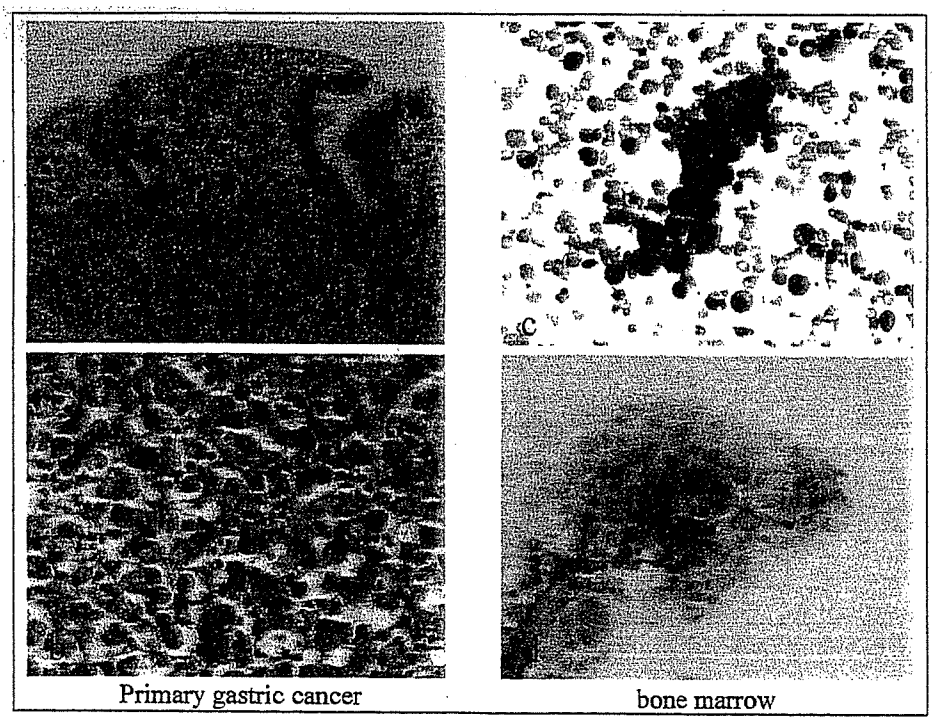

Figure 1. Photomicrographs of a primary gastric cancer specimen (a and b) and bone marrow aspiration smear (c and d) in disseminated carcinomatosis of the bone marrow (case 5). A gastric cancer specimen showed mucosal involvement by signet ring cell carcinoma cells (a, x20; b, x40; hematoxylin and eosin). A bone marrow aspiration smear showed metastatic infiltration by signet ring carcinoma cells (c, x40, Giemsa; d, x40, PAS).

patients had undergone prior surgery for gastric cancer before this condition was identified (cases 1-8 in Table I), and as a result, the diagnosis of gastric cancer was histologically proven in all 8 cases. In one patient (case 9 in Table I), on the other hand, the discovery of this condition preceded the diagnosis of gastric cancer, and the diagnosis was thus made based on the histological findings of the specimens obtained during a gastroendoscopic biopsy.